



Geophysical Research Letters*



RESEARCH LETTER

10.1029/2023GL106024

YuRui Li and Yang Zhang contributed equally to this work.

Key Points:

- The morphology of lightning channels can reflect the distribution of turbulence intensity, and a certain correlation between the two exist
- Directly extended lightning channels tend to propagate in the direction of decreasing eddy dissipation rates
- The location of the channel bifurcations or turns often corresponds to regions with high eddy dissipation rates

Supporting Information:

Supporting Information may be found in the online version of this article.

Correspondence to:

Y. Zhang and Y. Zhang, zhangyang@cma.gov.cn; zhangyijun@fudan.edu.cn

Citation:

Li, Y., Zhang, Y., Zhang, Y., & Krehbiel, P. R. (2024). Analysis of the relationship between the morphological characteristics of lightning channels and turbulent dynamics based on the localization of VHF radiation sources. *Geophysical Research Letters*, *51*, e2023GL106024. https://doi.org/10.1029/2023GL106024

Received 25 AUG 2023 Accepted 5 JAN 2024

© 2024. The Authors.

This is an open access article under the terms of the Creative Commons Attribution-NonCommercial-NoDerivs License, which permits use and distribution in any medium, provided the original work is properly cited, the use is non-commercial and no modifications or adaptations are made.

Analysis of the Relationship Between the Morphological Characteristics of Lightning Channels and Turbulent Dynamics Based on the Localization of VHF Radiation Sources

YuRui Li^{1,2}, Yang Zhang², YiJun Zhang^{1,3,4}, and Paul R. Krehbiel⁵

¹Department of Atmospheric and Oceanic Sciences and Institute of Atmospheric Sciences, Fudan University, Shanghai, China, ²State Key Laboratory of Severe Weather, Chinese Academy of Meteorological Sciences, Beijing, China, ³CMA-FDU Joint Laboratory of Marine Meteorology, Shanghai Frontiers Science Center of Atmosphere-Ocean Interaction, Shanghai, China, ⁴Shanghai Qi Zhi Institute, Shanghai, China, ⁵Langmuir Laboratory for Atmospheric Research, Geophysical Research Center, New Mexico Institute of Mining and Technology, Socorro, NM, USA

Abstract Lightning channel morphology depends on the thunderstorm cloud charge structure, which in turn is influenced by the thunderstorm dynamics. In this paper, based on three-dimensional radiation source localization data from the Lightning Mapping Array and radar-based data, our analysis shows that the overall morphology and detailed morphology of the lightning channel correspond to different eddy dissipation rate (EDR) characteristics. Lightning with complex channel morphology occurs in regions with large EDRs. In single lightning events, channels that extend directly within a certain height range without significant bifurcation and turning tend to propagate in the direction of decreasing EDRs, while channel bifurcations and turns usually occur in regions with large radial velocity gradients and large EDRs. This study shows the relationship between channel morphology and thunderstorm dynamics and provides a new method for the direct application of channel-level localization data to understand thunderstorm dynamics characteristics.

Plain Language Summary Turbulence in thunderstorms affects the charge distribution, which in turn affects the lightning channel morphology. Thus, the lightning channel morphology can reflect the characteristics of turbulence. The current understanding of the correlation between the two is still limited to the relationship between macroscopic thunderstorm dynamic characteristics and lightning activity. In this paper, the relationship between the morphology of the lightning channel and turbulence characteristics is investigated based on the Lightning Mapping Array (LMA) localization data and the cube root of the eddy dissipation rate (EDR) estimated from KABX radar-based data. The turbulence strength affects the overall morphology of lightning, and lightning with complex morphology tends to occur in regions with large EDRs. In single lightning events, channels extending directly within a certain altitude range tend to propagate in the direction of decreasing EDRs, and lightning channel bifurcation or turning tends to occur in regions with large EDRs. This paper establishes the relationship between thunderstorm electricity and thunderstorm dynamics by using lightning channel morphology as a bridge and provides a new method for the direct application of channel-level localization data to understand thunderstorm dynamics characteristics.

1. Introduction

The different morphologies of lightning channels are caused by different electrical environments within the cloud, the charge distribution determines the lightning channel morphology, and the lightning morphology can reflect the charge structure to some extent. Previously, the description of lightning morphology was usually based on the overall description of lightning. For example, Lu et al. (2012) classified lightning into four types: typical negative ground flash, Hybrid NCG-IC flash, Hybrid IC-NCG flash, and Bolt from the blue flash, or used the description of sprites as columns, carrots, jellyfish sprites and other different morphologies (Contreras-Vidal et al., 2021), without describing the channel morphology in detail from the perspective of a single lightning propagation process. Li et al. (2022) used the fractal dimension (FD) to describe the detailed features of the lightning channel bifurcation, turning and direct extension morphologies based on Lightning Mapping Array (LMA) radiation source localization with thunderstorm nonmissing detection capability and indicated that the lightning channel morphology could reflect more detailed horizontal charge structure characteristics in thunderstorm

clouds; the areas of lightning channel bifurcation and turning are areas of large charge density, and the areas of direct extension are less dense.

The distribution of charges is mainly determined by the dynamics and microphysical conditions in clouds, and recently, researchers have found that turbulence plays a significant role in the distribution of charges. Zhao et al. (2021) indicated that turbulence was fundamentally involved in the electrification process of thunderstorms. Turbulence in clouds could provide velocity differences for different masses and inertia of hydromorphic particles, which could affect the collisional velocity of hydromorphic particles in the mixed phase layer. Colgate (1967) studied the relationship between the hydrodynamic effect of electrostatic stress and the dynamics of thunderstorms and believed that turbulence generated by convective movement was a necessary condition for the formation of a strong electric field required for lightning initiation. Turbulence affects the charge density in clouds, and the change in charge density is also accompanied by enough turbulent stress to overcome electrostatic stress. Mareev and Dementyeva (2017) proposed that charge pockets could be caused by local turbulence, which could enhance local or established electric fields and lead to the generation of lightning. The eddy dissipation rate (EDR) is an important parameter to measure the intensity of turbulence and can be estimated from parameters, such as radial velocity and velocity spectral width, provided by Doppler radar (Bohne, 1982; Frisch & Strauch, 1976; Istok & Doviak, 1986). Frisch and Strauch (1976) reported turbulent kinetic energy dissipation rates in a thunderstorm measured with Doppler radar and showed that the EDR ranged from 0.03 m² s⁻³ to greater than $0.35\ m^2\ s^{-3}$ in the region between updrafts and downdrafts.

Due to the dependence of lightning morphology on the distribution of thunderstorm charges, which is regulated by thunderstorm dynamic effects, a relationship can be established between lightning morphology and thunderstorm dynamic effects. However, previous studies have not described lightning morphology in terms of the channel details, and most studies on the relationship between thunderstorm dynamical structure and lightning have focused on the overall characteristics of the lightning activity, such as lightning initiation, lightning scale and flash rate. Bryan et al. (2003) found that turbulent eddies tended to arise at the periphery or edge of the maximum updraft rise rate, where lightning often initiates and where there are large flash rates and flash extent densities around the updraft (Damiani et al., 2006; DiGangi et al., 2016). Calhoun et al. (2013) concluded that as the distance to the thunderstorm updraft increased, the flash rate decreased and the horizontal extension increased, with the smallest lightning commonly occurring in the hook echo and updraft regions. Bruning and MacGorman (2013) indicated that flash scale and flash rate were directly related to turbulence and that the flash scale and flash rate varied with thunderstorm hydrodynamics (Deierling & Petersen, 2008; Mecikalski et al., 2015; Schultz et al., 2015). Z. Zhang et al. (2017) found that lightning occurred on a small scale in updraft regions with strong convective motion in thunderstorm clouds and on a large scale in stratiform cloud regions at the cloud anvil. However, none of the above studies traced the dynamic structure of the lightning channel path in detail. In this paper, we use the lightning channel characterized by the LMA radiation sources and the radar-estimated EDR to examine the relationship between the overall morphology of the lightning channel, the different detailed channel morphologies of a single lightning event (direct extension, change in propagation direction, and bifurcation within a certain altitude range) and the turbulence characteristics within a thunderstorm cloud.

2. Data and Methods

In this study, the lightning channel was obtained from LMA radiation source localization data. The S-band dual-polarization Doppler radar data were used to estimate the cube root of the EDR (EDR in the later text refer to the cube root of the EDR). The EDR and radar radial velocity were used to represent the thunderstorm dynamic characteristics, and the EDR and radar radial velocity were superimposed on the LMA radiation sources to investigate the relationship between the channel morphology of lightning such as the direct extension, bifurcation, and turning within a certain altitude range and the dynamic characteristics inside the thunderstorm cloud.

2.1. Data

This study mainly analyzed the three-dimensional localization of VHF radiation source data of 23 lightning flashes in New Mexico, United States, from June to July 2014 and August 2015. The localization data were obtained from Lightning Mapping Array (LMA) observations at the Langmuir Laboratory of the New Mexico Institute of Mining and Technology. The LMA consisted of more than 20 substations, and the 3D localization possessed a temporal resolution of $80~\mu s$ and a positioning accuracy of tens of meters within the station network

LI ET AL. 2 of 10

(Rison et al., 1999; Thomas, 2004; Y. Zhang et al., 2006a, 2006b). In this study, strict selection criteria (number of stations ≥ 7 ; reduced chi-square values ≤ 2) were used to ensure the reliability of the localization data. All lightning occurrences were concentrated within the east-west 64 km and north-south 48 km range of the station network, with high localization accuracy. The lightning flashes analyzed here are all within the detection range of KABX rada in Albuquerque, New Mexico. The radar is located approximately 130 km east-northwest of the center of the LMA. Its scans generally have 14 layers of elevation angles of 0.5°, 0.9°, 1.3°, 1.8°, 2.4°, 3.1°, 4.0°, 5.0° , 6.4° , 8.0° , 10.0° , 12.5° , 15.5° , 19.5° , and the beam width of about 1° . The radial range gate is 250 m. The beam broadening depends on the distance from the radar. The maximum distance between the lightning cases used in this study and the KABX radar is ~138 km, and the minimum distance is ~99 km. The radar beam broadening range corresponding to the lightning case in this study is 1.74-2.41 km. The relationship between the overall morphology of the lightning channel and turbulence characteristics was discussed by using 23 lightning cases (In the main text, we use two individual examples of lightning that occurred at 21:53:30 on 15 July 2014, and 19:14:17 on 13 June 2014 (referred to later as Flash 1 and Flash 2, respectively) to illustrate). The FDs and average EDRs of the channel regions for the other lightning examples are shown in Table S2 in Supporting Information \$1. The relationship between the detailed morphology of the lightning channel and turbulence characteristics was discussed using five lightning examples that occurred at 23:23:21 on 30 June 2014, 23:28:34 on 30 June 2014, 21:50:05 on 15 July 2014, 19:35:22 on 13 June 2014, and 21:52:13 on 15 July 2014 (hereafter referred to as Flash 3 Flash 4, Flash 5, Flash 6, and Flash 7; see Table S1 in Supporting Information S1 for the lightning information).

2.2. Calculation of Eddy Dissipation Rate and Lightning Overall Morphological Characterization Parameter

The Python ARM Radar Toolkit (Py-ART) (Helmus & Collis, 2016) was used to process the radar data. The EDR was estimated using the Python Turbulence Detection Algorithm (pyTDA) (Lang & Guy, 2017), which calculated the cube root of the EDR through the input radar data (including reflectivity and velocity spectral width) and could provide a three-dimensional turbulence distribution. Since interpolation affected the accuracy of radar data, we directly use polar coordinate data. Therefore, the resolution of EDR is consistent with that of radar.

The geometry of lightning is fractal (Riousset et al., 2007; Vecchi et al., 1994), and the FD can characterize the complexity of lightning channels and quantitatively describe the morphology of lightning channels (Li et al., 2022). The box-counting method was used to calculate the FD of each lightning (see Maragos and Fan-Kon (1993) for details) with the following formula:

$$FD = \lim_{\epsilon \to 0} \frac{\log N(\epsilon)}{\log \frac{1}{\epsilon}}$$

where FD is the fractal dimension, ε is the edge length of the box, and N is the number of boxes covered. FD reflects the effectiveness of the space occupied by the complex form, while the scale of each lightning (here denoted by the convex hull area (S)) is different. Therefore, when measuring the complexity of a lightning channel morphology, the FD per unit area should be used. We adopt a new parameter (T), which is calculated as:

$$T = \frac{\text{FD}}{S}$$

Where *S* is the convex hull area of the lightning, calculated using the convhull function of *MATLAB* (a registered trademark of The MathWorks, Inc.). In this paper, *T* is used to measure the overall morphological complexity of each lightning channel.

2.3. Matching Between Lightning Radiation Sources and EDRs

The EDR data for each elevation angle corresponds to a certain range, and this range is different at different locations. In order to superimpose the EDR and lightning channels for analysis, we need to match the lightning radiation source to the EDR, and the matching method is as follows:

Firstly, calculate the average position of lightning cases. Then, calculate the distance r between the lightning case and the radar:

 $r = R \times arc \cos(\cos(\text{lat}_{ave}) \times \cos(\text{lat}_{radar}) \times \cos(\text{lon}_{ave} - \text{lon}_{radar}) + \sin(\text{lat}_{ave}) \times \sin(\text{lat}_{radar}))$

LI ET AL. 3 of 10

where R is the radius of the Earth, lon_{radar} and lat_{radar} are the radar longitude and latitude, lon_{ave} and lat_{ave} is the average longitude and latitude of lightning case.

It should be noted that the elevation angle we refer to is actually the center elevation angle of the beam, and the radar beam width is approximately 1°. When the elevation angle is α , its actual detection range is $\alpha - 0.5^{\circ}$ to $\alpha + 0.5^{\circ}$. (For example, data with an elevation angle of 4.0° actually detects a range of $4.0^{\circ} \pm 0.5^{\circ}$ (i.e., $3.5^{\circ}-4.5^{\circ}$)).

Next, the height range $h_{\text{range}}(h_{\text{min}} \text{ to } h_{\text{max}})$ corresponding to the beam at each radar elevation angle is calculated at the lightning average position, where

$$h_{\min} = r \times \sin(\alpha - 0.5) + h_{\text{radar}}$$

$$h_{\text{max}} = r \times \sin(\alpha + 0.5) + h_{\text{radar}}$$

where α is the elevation angle and h_{radar} is the radar altitude. Finally, the lightning radiation sources within this altitude range are superimposed with the cube root of the EDR at this elevation angle to obtain the correspondence between the lightning channel and the EDR.

3. Results

3.1. Lightning Overall Morphology and Turbulence Characteristics

When comparing the overall morphology of different lightning, we use the parameter T to represent the complexity of the lightning channel (see Section 2.2 for specific calculation method). In general, the larger T is, the greater the lightning channel occupies per unit area, and the more complex the channel is, with more bifurcations and turns; the smaller T is, the smaller the lightning channel occupies per unit area, and the simpler the channel is, with a greater tendency to extend directly in one direction. We calculated the T of the 23 flashes and the average cube of EDR of the area where the flashes are located (see Table S2 in Supporting Information S1 for the T and the cube of the EDR). T and EDR were found to exhibit some degree of positive correlation, with a correlation coefficient of 0.46, and passed a significance test with a significance level of 0.05 (p-value of 0.01). Taking Flash 1 and Flash 2 as examples, we analyze in detail the differences in the lightning overall morphology and turbulence characteristics of the lightning channel region for large and small T values. Figure 1 shows the horizontal projections of the radiation sources and the EDR of the channel regions of Flash 1 and Flash 2. The channel of Flash 1 was more complex with more branches, the parameter T is 2.16, the mean value of the EDR of the channel region was 0.3 (m² s⁻³)^{1/3}; while the channel of Flash 2 had a simpler morphology, the parameter T is 1.97, the mean value of the EDR of the channel region was 0.2 (m² s⁻³)^{1/3}. Regions with large EDRs have more complex lightning channel overall morphologies. Taking a lightning as a whole, we found a correlation between the overall morphology of the lightning channel and the EDR. Considering EDR may be affected by factors such as height and in order to obtain a more rigorous and detailed relationship, we will explore the effect of local small-area EDR on the detailed morphology of the lightning channel in the following section.

3.2. Turbulence Characteristics of Direct Extended Channels

We used Flash 3 and Flash 4 as examples to analyze the turbulence characteristics of the direct extension channel of lightning. Figure 2 shows the radiation source distributions of Flash 3 and Flash 4 and the superposition with the EDR distributions. As shown in Figures 2a and 2c, the continuous propagation channel of interest in Flash 3 within an altitude range of 9–10 km initiated near (–107.00, 33.91) and extended roughly in a north direction, with no apparent change in direction or bifurcation during propagation. As shown in Figure 2e and the black lines in Figure 2g, the EDR gradually decreased as the channel extended directly and away from the initiation position. As shown in Figures 2b and 2d, the channel of interest in Flash 4 initiated near (–106.99, 33.89) and then continuously propagated to the northeast within an altitude range of 9–10 km, and there was no significant turning or bifurcation during the direct extension of the channel. As shown in Figure 2f and the red lines in Figure 2g, the EDR also gradually decreased. Figure S1 in Supporting Information S1 shows the trend of the EDR changes during the channel propagation process of many other lightning cases. Lightning channels propagating horizontally and continuously within a certain height range tended to propagate in the direction of decreasing EDRs, with decreasing rates ranging from 0.01 (m² s⁻³)^{1/3}/km to 0.03 (m² s⁻³)^{1/3}/km; this result was consistent with Souza and Bruning's (2021) deductions that greater turbulence intensity was associated with a

LI ET AL. 4 of 10

Institute Of Mining And Technology, Wiley Online Library on [21/01/2024]. See the Term

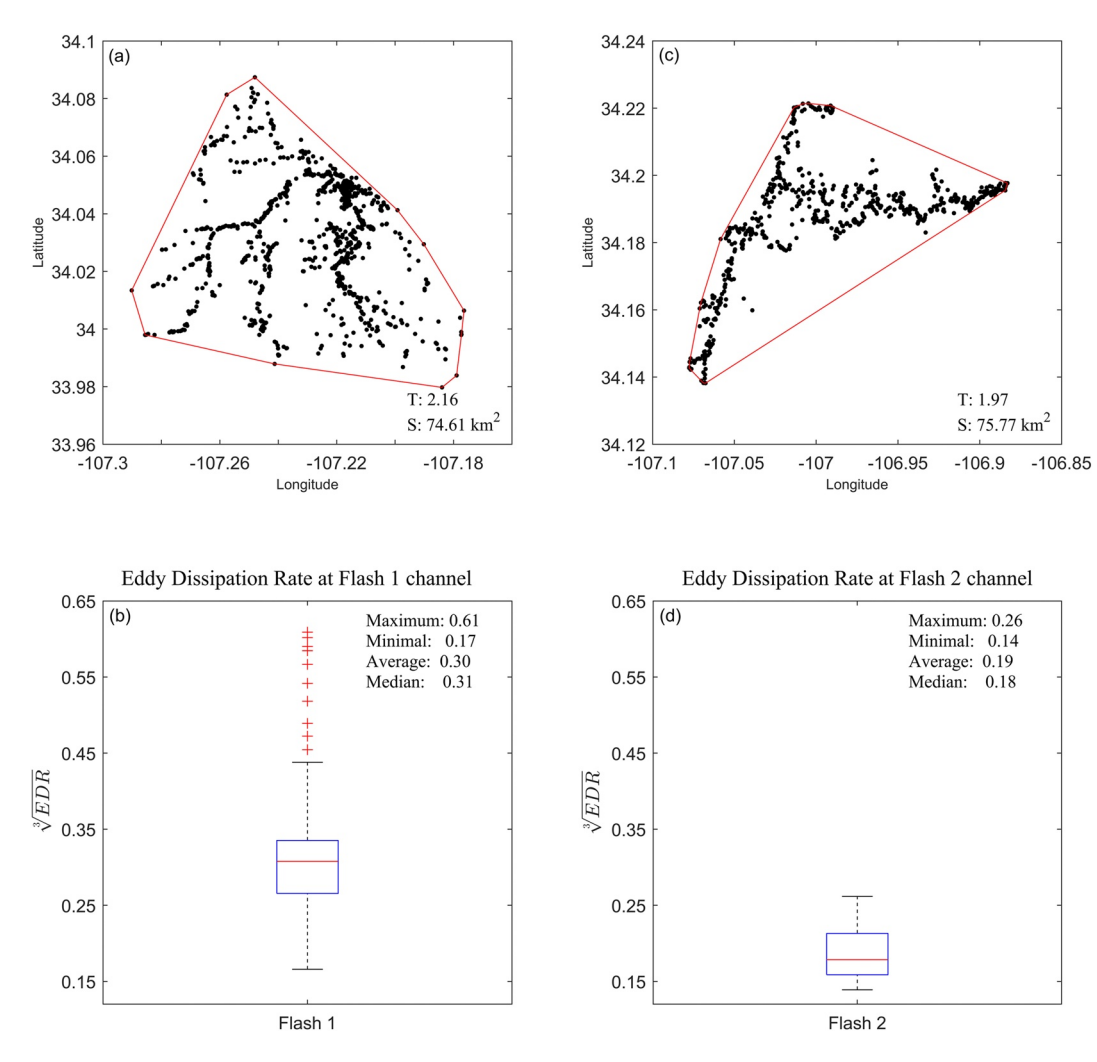


Figure 1. (a) Horizontal projection of Flash 1 radiation source; (b) EDR of Flash 1 channel area; (c) Horizontal projection of Flash 2 radiation source; (d) EDR of Flash 2 channel area.

decreasing distance from the location of lightning initiation. The size of the EDR could affect the ionization of the channel and thus the velocity of leader development. This was corroborated by the study of Jensen et al. (2021). They found that the velocity of the lightning leader during k progress decreased as it returned along the already ionized channel, probably due to the larger EDR accelerating electron convergence and increasing the resistance. However, the EDR did not always decrease strictly throughout the propagation of the lightning channel but also fluctuated, and these fluctuations corresponded to changes in the morphology of the lightning channel, which are explored in the following section.

3.3. Local Dynamical Characteristics of Lightning Channel Turning and Bifurcation

The relationship between complex lightning channel morphology (turning and bifurcation) and the dynamical characteristics of thunderstorm clouds are further investigated here, and three examples, Flash 5, Flash 6, and Flash 7, are selected for detailed analysis. Results for other lightning cases with obvious turning and bifurcation are shown in Figure S2 in Supporting Information S1. As shown in Figures 3d and 3g, the channel of flash 5 at an altitude of 6–8 km propagates roughly to the west and bifurcates near (–107.24, 34.02) (white box A in Figure 3g) to the northwest and southwest, respectively. From the red line in Figure 3j, there is an extreme value of the EDR at region A, which is approximately 0.4 (m² s⁻³)^{1/3}, and after passing through region A, the channel propagates in the direction of decreasing EDR. The channel of Flash 6 at 8–10 km altitude initially propagates southwestward (Figures 3b and 3e). The direction of channel development changes in region B and then

LI ET AL. 5 of 10

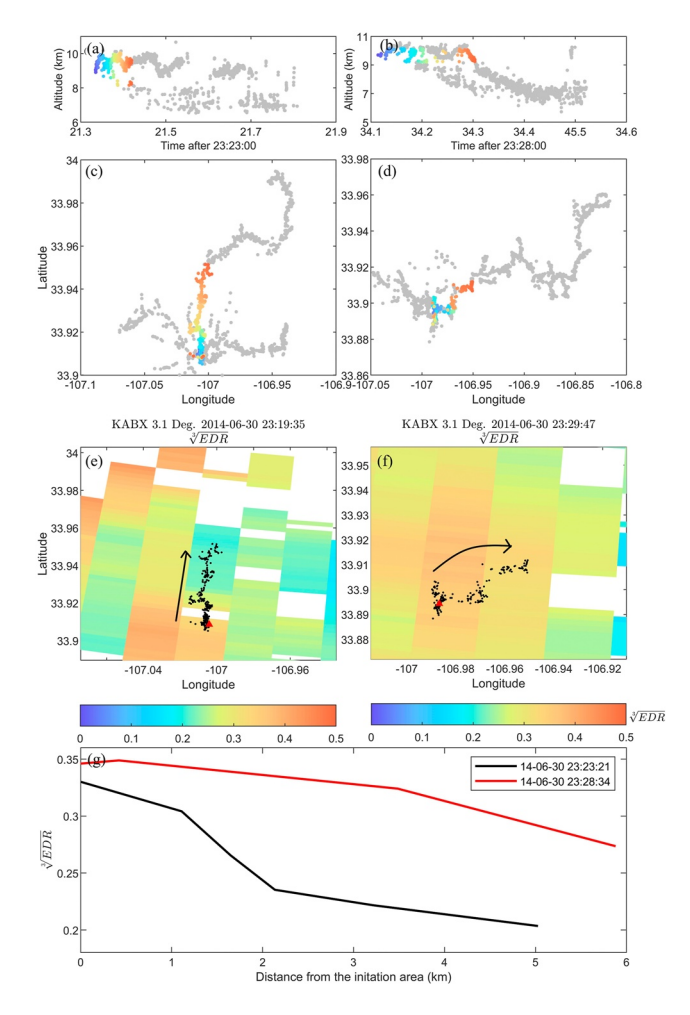


Figure 2. (a)—(b) Time-height distribution of Flash 3 and Flash 4; (c)—(d) Planar projection of Flash 3 and Flash 4; the gray dots represent the entire lightning radiation source, the colored dots represent the lightning channels of interest that develop continuously within a range of altitudes, and the radiation sources are colored by time; (e)—(f) Superimposed EDR distribution of flash 3 and flash 4 radiation sources; the black dots indicate the lightning radiation source, the shaded diagrams represent the EDR, the red triangle represents the initiation position of the lightning, and the black arrow represents the development direction of the channel; (g) Variation in the EDR with distance during the direct extension of the channel for Flash 3 (black) and Flash 4 (red).

propagates westward (Figure 3h), accompanied by a sudden increase in the EDR (green line in Figure 3j) of approximately 0.3 (m² s⁻³)^{1/3}, and then the channel continues to propagate westward with a decrease in the EDR. The channel of Flash 7 roughly propagates southward within the 6-8 km altitude (Figures 3c and 3f), bifurcating at region C in Figure 3i, where the EDR is also large, approximately 0.3 (m² s⁻³)^{1/3}, and then propagates toward a decreasing EDR. Based on the above results, lightning channel bifurcation or turning always occurs in the region with a larger EDR. In addition, there are positive and negative velocity pairs in regions A, B, and C. As shown in Figure 4a, the bifurcation region of Flash 5 (region A), the turning region of Flash 6 (region B), and the bifurcation region of Flash 7 (region C) are all located in the region of the positive-negative velocity pairs, which corresponds to the upward or downward movement of the flow and larger relative motion of the particles. These regions have a larger EDR and stronger dynamics, which may cause the charge structure to become more fragmented, forming small pocket charge regions and multiple localized large-value regions of the electric field. The morphology of the lightning channels changes when subjected to the electric field during development, bifurcation, or turning in these regions. Our study shows that the lightning channel morphology can reflect thunderstorm dynamic characteristics. Although previous authors have also focused on the relationship between lightning activity and thunderstorm dynamics, they have mainly concentrated on macroscopic aspects, such as the dynamic effect and lightning scale (convex hull area), flash rate, flash density, and flash initial density (Calhoun et al., 2013; Z. Zhang et al., 2017; Zheng et al., 2019). Due to the limitations of observational data, there is still no in-depth conclusion on the relationship between lightning channels and thunderstorm dynamics. Li et al. (2022) indicated that the morphology of the lightning channel (bifurcation and turning) could reflect the charge structure of thunderstorms, and in this paper, we further used the morphology of the lightning channel as a bridge to build a connection between thunderstorm electricity and thunderstorm dynamics.

4. Conclusion and Discussion

Based on LMA radiation source localization data for 23 flashes in New Mexico in August 2013 and June–July 2014 and the EDR estimated from KABX radar data, the relationship between the overall morphology of the lightning channel, as well as the detailed morphology of the lightning channel within a range of altitudes in a single flash, and the local dynamical characteristics within the thunderstorm cloud was examined, and the main findings are as follows:

- 1. As a whole, the turbulence strength affects the overall morphology of the lightning channel, and lightning with complex channel morphology and large *T* often occurs in regions with large EDRs; lightning with simple channel morphology and small *T* occurs in regions with small EDRs.
- From a local perspective, for lightning channels that directly extend within a range of heights, with no significant change in propagation direction and no evident bifurcation, the EDR decreases as the channel extends, and the direction of extension is generally the direction in which the EDR decreases.
- 3. From a local perspective, lightning channels that continuously propagate within a range of altitudes have larger EDRs in the region of bifurcation and turning; this is a region where there are positive and negative velocity pairs of radial velocities, large velocity gradients, and strong dynamics.

For conclusion 1, it just established a rough relationship between the overall lightning channel and EDR. Based on this general relationship, we further investigated a more rigorous relationship between the detailed morphology of lightning channels and EDR. For conclusions 2 and 3, it is more suitable for lightning channels continuously

LI ET AL. 6 of 10

19448007, 2024. 2, Downloaded from https://agupubs.onlinelibrary.wiley.com/doi/10.1029/2023GL106024 by New Mexico Institute Of Mining And Technology, Wiley Online Library on [21/01/2024]. See the Terms

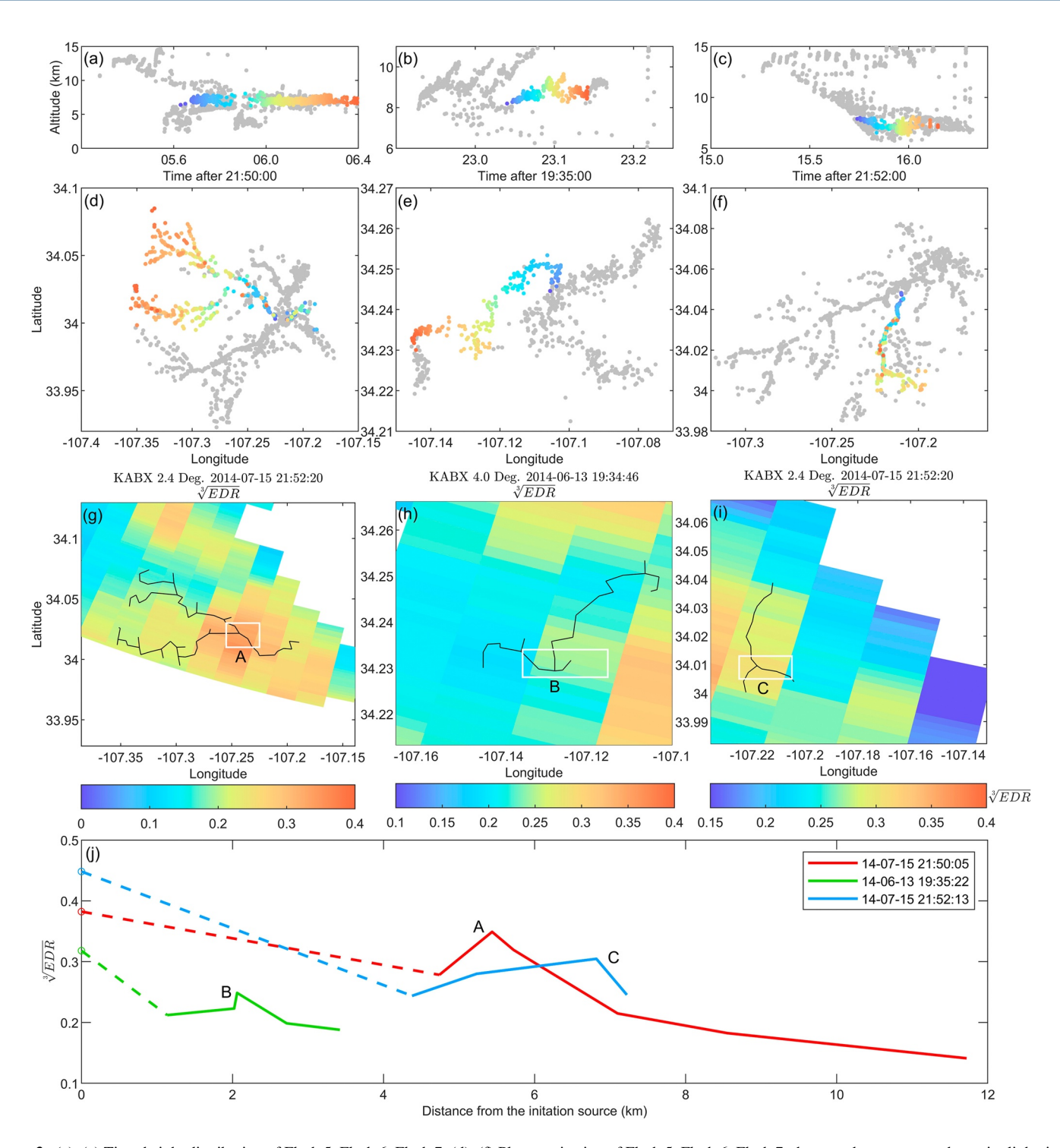


Figure 3. (a)–(c) Time-height distribution of Flash 5, Flash 6, Flash 7; (d)–(f) Plane projection of Flash 5, Flash 6, Flash 7; the gray dots represent the entire lightning radiation source, the colored dots represent the lightning channels of interest that continuously develop within a range of altitudes, and the radiation sources are colored by time; (g)–(i) Superimposed EDR distribution of Flash 5, Flash 6 and Flash 7 radiation sources; the white box A, B, C show the area of channel bifurcation or turning, the black dots indicate the lightning radiation source, and the shaded diagrams represent the EDR; (j) Variation of the EDR with distance during channel propagation for Flash 5 (red), Flash 6 (green) and Flash 7 (blue). The hollow circles represent the EDR of the lightning initiation regions, and the dashed lines represent the regions that do not develop in a height range.

LI ET AL. 7 of 10

wiley.com/doi/10.1029/2023GL106024 by New Mexico

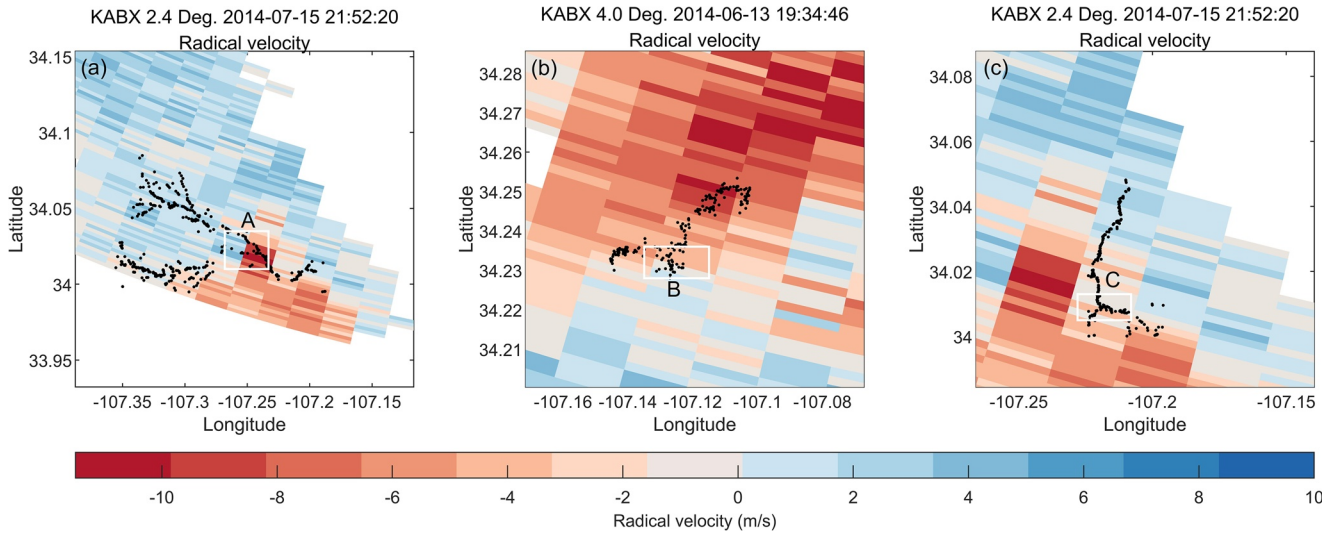


Figure 4. (a)—(c) Superimposed radial velocity distributions of the flash 5, flash 6, and flash 7 radiation sources. The white boxes A, B, and C show the areas of channel bifurcation or turning, the black dots indicate the lightning radiation source, and the shaded diagrams represent the radial velocities.

propagate within a certain height range. Otherwise, the EDR in the area where the channel occurs earlier is smaller than that in the area where the channel occurs later. This is illustrated by the example of the initiation region and the subsequent successive propagation region of Flash 1 (Figure S3 in Supporting Information S1); here, the spatial-temporal intervals between the initiation and successive propagation regions are ~100 ms and 3 km vertically, respectively, and the EDR in the initiation region is less than 0.3 (m² s⁻³)^{1/3}. However, the maximum EDR in the subsequent successive propagation region is greater than 0.3 (m² s⁻³)^{1/3}. This is potentially related to the large spatial-temporal intervals between the front and back channel regions. A lightning process usually lasts a few hundred milliseconds and develops horizontally over tens of kilometers and vertically over thousands of meters across different layers of charge. In terms of time, for channels that develop discontinuously and undergo long time intervals after initiation, the EDR of the selected propagation region significantly changes due to the rapid change in the EDR (Frisch & Strauch, 1976). In terms of spatial scale, there is significant variability in EDR at different altitudes. As shown in Figure S4 in Supporting Information S1, the center of the 45-dBZ reflectivity at two location of the initiation and the successive development of the subsequent channel both extends to 8.8 km. However, the initiation process of Flash 1 is in the 11-14 km altitude range and the successive development of the subsequent channel is in the 6-8 km altitude range. There is a stronger updraft in the region of the subsequently developed channel (MacGorman & Nielsen, 1991) and there is a more turbulent eddy generated in the periphery of the stronger updraft (Salinas et al., 2022), which may lead to a higher EDR. In addition, the conclusions of this paper apply to large-scale lightning channels. For small-scale discharge, such as space leaders, it is difficult to analyze such discharge processes in the current resolution of EDR, and LMA is also difficult to detect them. The study of the relationship between EDR and such discharge may require the use of phased array radar with higher spatial and temporal resolution to match the optical or interferometer data of lightning (Jiang et al., 2017; Pu & Cummer, 2024; Y. Zhang et al., 2017).

In addition, previous studies have indicated that lightning with smaller scales is usually produced in regions with stronger thunderstorm dynamics and larger EDRs (Souza & Bruning, 2021; Z. Zhang et al., 2017). However, in this paper, we found that in regions with strong turbulence, the channel morphology is more complex, and channel branching is more abundant, which in turn increases the lightning discharge scale (Li et al., 2021). Although lightning covers a smaller area in these regions, the discharge scales may not be small due to the presence of bifurcations.

Data Availability Statement

This work complies with the AGU data policy. The radar data used in this paper is available at Li (2023b). The LMA data used in this paper is available at Li (2023a).

LI ET AL. 8 of 10

Acknowledgments

This research was funded by the National Natural Science Foundation of China (42175090, U2342215), National Key Research and Development Program of China (2019YFC1510103), S&T Development Fund of CAMS (2023KJ050), the Basic Research Fund of Chinese Academy of Meteorological Sciences (Grants 2021Z011, 2023Z008). We are very grateful to the lightning team of NMT for providing LMA data. And also thank the Radar Operations Center of NOAA's National Weather Service which shares the radar data of New Mexico.

References

- Bohne, A. R. (1982). Radar detection of turbulence in precipitation environments. *Journal of the Atmospheric Sciences*, 39(8), 1819–1837. https://doi.org/10.1175/1520-0469(1982)039<1819:rdotip>2.0.co;2
- Bruning, E. C., & MacGorman, D. R. (2013). Theory and observations of controls on lightning flash size spectra. *Journal of the Atmospheric Sciences*, 70(12), 4012–4029. https://doi.org/10.1175/jas-d-12-0289.1
- Bryan, G. H., Wyngaard, J. C., & Fritsch, J. M. (2003). Resolution requirements for the simulation of deep moist convection. *Monthly Weather Review*, 131(10), 2394–2416. https://doi.org/10.1175/1520-0493(2003)131<2394:rrftso>2.0.co;2
- Calhoun, K. M., MacGorman, D. R., Ziegler, C. L., & Biggerstaff, M. I. (2013). Evolution of lightning activity and storm charge relative to dual-doppler analysis of a high-precipitation supercell storm. *Monthly Weather Review*, 141(7), 2199–2223. https://doi.org/10.1175/ mwr-d-12-00258.1
- Colgate, S. A. (1967). Enhanced drop coalescence by electric fields in equilibrium with turbulence. *Journal of Geophysical Research*, 72(2), 479–487. https://doi.org/10.1029/jz072i002p00479
- Contreras-Vidal, L., Sonnenfeld, R. G., da Silva, C. L., McHarg, M. G., Jensen, D., Harley, J., et al. (2021). Relationship between sprite current and morphology. *Journal of Geophysical Research: Space Physics*, 126(3), e2020JA028930. https://doi.org/10.1029/2020ja028930
- Damiani, R., Vali, G., & Haimov, S. (2006). The structure of thermals in cumulus from airborne dual-doppler radar observations. *Journal of the Atmospheric Sciences*, 63(5), 1432–1450. https://doi.org/10.1175/jas3701.1
- Deierling, W., & Petersen, W. A. (2008). Total lightning activity as an indicator of updraft characteristics. *Journal of Geophysical Research*, 113(D16), D16210. https://doi.org/10.1029/2007jd009598
- DiGangi, E. A., MacGorman, D. R., Ziegler, C. L., Betten, D., Biggerstaff, M., Bowlan, M., & Potvin, C. K. (2016). An overview of the 29 May 2012 Kingfisher supercell during DC3. *Journal of Geophysical Research: Atmospheres*, 121(24), 14316–314343. https://doi.org/10.1002/2016jd025690
- Frisch, A. S., & Strauch, R. G. (1976). Doppler radar measurements of turbulent kinetic energy dissipation rates in a northeastern Colorado convective storm. *Journal of Applied Meteorology*, 15(9), 1012–1017. https://doi.org/10.1175/1520-0450(1976)015<1012:drmotk>2.0.co;2
- Helmus, J. J., & Collis, S. M. (2016). The python ARM radar toolkit (Py-ART), a library for working with weather radar data in the python programming language. *Journal of Open Research Software*, 4(1), e25. https://doi.org/10.5334/jors.119
- Istok, M. J., & Doviak, R. J. (1986). Analysis of the relation between doppler spectral width and thunderstorm turbulence. *Journal of the Atmospheric Sciences*, 43(20), 2199–2214. https://doi.org/10.1175/1520-0469(1986)043<2199:aotrbd>2.0.co;2
- Jensen, D. P., Sonnenfeld, R. G., Stanley, M. A., Edens, H. E., da Silva, C. L., & Krehbiel, P. R. (2021). Dart-leader and k-leader velocity from initiation site to termination time-resolved with 3d interferometry. *Journal of Geophysical Research: Atmospheres*, 126(9), e2020JD034309. https://doi.org/10.1029/2020JD034309
- Jiang, R., Qie, X., Zhang, H., Liu, M., Sun, Z., Lu, G., et al. (2017). Channel branching and zigzagging in negative cloud-to-ground lightning. Scientific Reports, 7(1), 3457. https://doi.org/10.1038/s41598-017-03686-w
- Lang, T. J., & Guy, N. (2017). Diagnosing turbulence for research aircraft safety using open source toolkits. Results in Physics, 7, 2425–2426. https://doi.org/10.1016/j.rinp.2017.07.015
- Li, Y. (2023a). LMA data [Dataset]. Zenodo. https://doi.org/10.5281/zenodo.8237716
- Li, Y. (2023b). Radar data [Dataset]. Zenodo. https://doi.org/10.5281/zenodo.10238886
- Li, Y., Zhang, Y., Zhang, Y., & Krehbiel, P. R. (2021). A new method for connecting the radiation sources of lightning discharge extension channels. *Earth and Space Science*, 8(7), e2021EA001713. https://doi.org/10.1029/2021ea001713
- Li, Y., Zhang, Y., Zhang, Y., & Krehbiel, P. R. (2022). Analysis of the configuration relationship between the morphological characteristics of lightning channels and the charge structure based on the localization of VHF radiation sources. *Geophysical Research Letters*, 49(15), e2022GL099586. https://doi.org/10.1029/2022gl099586
- Lu, G., Cummer, S. A., Blakeslee, R. J., Weiss, S., & Beasley, W. H. (2012). Lightning morphology and impulse charge moment change of high peak current negative strokes. *Journal of Geophysical Research*, 117(D4), D04212. https://doi.org/10.1029/2011jd016890
- MacGorman, D. R., & Nielsen, K. E. (1991). Cloud-to-ground lightning in a tornadic storm on 8 May 1986. Monthly Weather Review, 119(7), 1557–1574. https://doi.org/10.1175/1520-0493(1991)119<1557:ctglia>2.0.co;2
- Maragos, P., & Fan-Kon, S. (1993). Measuring the fractal dimension of signals: Morphological covers and iterative optimization. IEEE Transactions on Signal Processing, 41(1), 108. https://doi.org/10.1109/tsp.1993.193131
- Mareev, E. A., & Dementyeva, S. O. (2017). The role of turbulence in thunderstorm, snowstorm, and dust storm electrification. *Journal of Geophysical Research: Atmospheres*, 122(13), 6976–6988. https://doi.org/10.1002/2016jd026150
- Mecikalski, R. M., Bain, A. L., & Carey, L. D. (2015). Radar and lightning observations of deep moist convection across northern Alabama during DC3: 21 May 2012. Monthly Weather Review, 143(7), 2774–2794. https://doi.org/10.1175/mwr-d-14-00250.1
- Pu, Y., & Cummer, S. A. (2024). Imaging step formation in in-cloud lightning initial development with VHF interferometry. *Geophysical Research Letters*, 51(1), e2023GL107388. https://doi.org/10.1029/2023g1107388
- Riousset, J. A., Pasko, V. P., Krehbiel, P. R., Thomas, R. J., & Rison, W. (2007). Three-dimensional fractal modeling of intracloud lightning discharge in a New Mexico thunderstorm and comparison with lightning mapping observations. *Journal of Geophysical Research*, 112(D15), D15203. https://doi.org/10.1029/2006jd007621
- Rison, W., Thomas, R. J., Krehbiel, P. R., Hamlin, T., & Harlin, J. (1999). A GPS-based three-dimensional lightning mapping system: Initial observations in central New Mexico. *Geophysical Research Letters*, 26(23), 3573–3576. https://doi.org/10.1029/1999gl010856
- Salinas, V., Bruning, E. C., & Mansell, E. R. (2022). Examining the kinematic structures within which lightning flashes are initiated using a cloud-resolving model. *Journal of the Atmospheric Sciences*, 79(2), 513–530. https://doi.org/10.1175/jas-d-21-0132.1
- Schultz, C. J., Carey, L. D., Schultz, E. V., & Blakeslee, R. J. (2015). Insight into the kinematic and microphysical processes that control lightning jumps. Weather and Forecasting, 30(6), 1591–1621. https://doi.org/10.1175/waf-d-14-00147.1
- Souza, J. C. S., & Bruning, E. C. (2021). Assessment of turbulence intensity in different spots of lightning flash propagation. *Geophysical Research Letters*, 48(21), e2021GL095923. https://doi.org/10.1029/2021gl095923
- Thomas, R. J., Krehbiel, P. R., Rison, W., Hunyady, S. J., Winn, W. P., Hamlin, T., & Harlin, J. (2004). Accuracy of the lightning mapping array. Journal of Geophysical Research, 109(D14), D14207. https://doi.org/10.1029/2004jd004549
- Vecchi, G., Labate, D., & Canavero, F. (1994). Fractal approach to lightning radiation on a tortuous channel. Radio Science, 29(4), 691–704. https://doi.org/10.1029/93rs03030
- Zhang, Y., Krehbiel, P. R., Zhang, Y., Lu, W., Zheng, D., Xu, L., & Huang, Z. (2017). Observations of the initial stage of a rocket-and-wire-triggered lightning discharge. *Geophysical Research Letters*, 44(9), 4332–4340. https://doi.org/10.1002/2017gl072843

LI ET AL. 9 of 10

- Zhang, Y., Meng, Q., Lu, W., Paul, K., Liu, X., & Zhou, X. (2006a). Charge structures and cloud-to-ground lightning discharges characteristics in two supercell thunderstorms. Chinese Science Bulletin, 51(2), 198–212. https://doi.org/10.1007/s11434-005-0233-7
- Zhang, Y., Meng, Q., Paul, K., Liu, X., Yan, M., & Zhou, X. (2006b). Spatiotemporal characteristics of positive cloud-to-ground lightning discharges and bidirectional leader of the lightning. Science in China Series D, 49(2), 212–224. https://doi.org/10.1007/s11430-005-0054-1
- Zhang, Z., Zheng, D., Zhang, Y., & Lu, G. (2017). Spatial–temporal characteristics of lightning flash size in a supercell storm. Atmospheric Research, 197, 201–210. https://doi.org/10.1016/j.atmosres.2017.06.029
- Zhao, C., Zheng, D., Zhang, Y., Liu, X., Zhang, Y., Yao, W., & Zhang, W. (2021). Turbulence characteristics of thunderstorms before the first flash in comparison to non-thunderstorms. *Geophysical Research Letters*, 48(18), e2021GL094821. https://doi.org/10.1029/2021gl094821
- Zheng, D., Wang, D., Zhang, Y., Wu, T., & Takagi, N. (2019). Charge Regions Indicated by LMA lightning flashes in Hokuriku's winter thunder-storms. *Journal of Geophysical Research: Atmospheres*, 124(13), 7179–7206. https://doi.org/10.1029/2018jd030060

LI ET AL. 10 of 10